Battery-Management System (BMS) and SOC Development for Electrical Vehicles

K. W. E. Cheng, *Senior Member, IEEE*, B. P. Divakar, Hongjie Wu, Kai Ding, and Ho Fai Ho

***Abstract*—Battery monitoring is vital for most electric vehicles (EVs), because the safety, operation, and even the life of the passenger depends on the battery system. This attribute is exactly the major function of the battery-management system (BMS)—to check and control the status of battery within their specified safe operating conditions. In this paper, a typical BMS block diagram has been proposed using various functional blocks. The state of charge (SOC) estimation has been implemented using Coulomb counting and open-circuit voltage methods, thereby eliminating the limitation of the stand-alone Coulomb counting method. By modeling the battery with SOC as one of the state variables, SOC can be estimated, which is further corrected by the Kalman filtering method. The battery parameters from experimental results are integrated in the model, and simulation results are validated by experiment.**

***Index Terms*—Battery-management system (BMS), electric vehicles (EVs), state of charge (SOC).**

NOMENCLATURE

Li-ion	Lithium ion.
$LiFePO_4$	Lithium-ion iron phosphate.
BMS	Battery-management system.
EV	Electric vehicle.
HEV	Hybrid electric vehicle.
OCV	Open-circuit voltage.
CAN	Control area network.
ECU	Electronic control unit.
EMF	Electromotive force.
SOC	State of charge.
SOH	State of health.
SOP	State of polarization.
E0	Constant voltage.
K	Polarization constant.
C	Polarization coefficients.
B	Exponential capacity $(\mathrm{Ah})^{-1}$.
A	Exponential voltage.
i	Current.
α, β, and γ	Polarization coefficients.
$\mathrm{Q_d}$	Double-layer capacity (in ampere-hours).
$\mathrm{R_n}$	Internal resistance (in ohms).
$\mathrm{I_k}$	Current (in amperes), which is positive when charged and negative when discharged [range: $(-500 \sim +500)$, according to the manufacturer].
$\Delta \mathrm{t}$	Sample period (in seconds).
$\mathrm{Q_R}$	Rated capacity (in ampere-hours).
M	Maximum polarization voltage (in volts).

Manuscript received July 31, 2009; revised December 3, 2009, March 23, 2010, June 9, 2010, and August 11, 2010; accepted August 31, 2010. Date of publication October 25, 2010; date of current version January 20, 2011. This work was supported in part by the Niche Areas Funding Scheme of the Hong Kong Polytechnic University under Project 1-BB86 and by the Automotive Parts and Accessory Systems R&D Centre Limited, under Project ITP-032-07AP, established with funding from the Innovation and Technology Fund, Hong Kong. The review of this paper was coordinated by Mr. D. Diallo.

K. W. E. Cheng and K. Ding are with the Power Electronics Research Centre, Department of Electrical Engineering, The Hong Kong Polytechnic University, Kowloon, Hong Kong (e-mail: eeecheng@polyu.edu.hk; eekding@polyu.edu.hk).

B. P. Divakar is with the Department of Electrical and Electronics Engineering, Reva Institute of Technology and Management, Bangalore 560064, India (e-mail: eebpdiva@hotmail.com).

H. Wu is with the National Engineering Laboratory of Automotive Electronics, Shanghai Jiao Tong University, Shanghai 200240, China (e-mail: wuhongjie@sjtu.edu.cn).

H. F. Ho is with the Department of Electrical Engineering, The Hong Kong Polytechnic University, Kowloon, Hong Kong (e-mail: eehfho@polyu.edu.hk).

Color versions of one or more of the figures in this paper are available online at http://ieeexplore.ieee.org.

Digital Object Identifier 10.1109/TVT.2010.2089647

I. INTRODUCTION

BATTERIES are the most common electrical energy-storage devices in EVs. The performance of a battery when it is connected to a load or a source is based on the chemical reactions inside the battery. The chemicals degrade with time and usage that reflect the gradual reduction in the energy storage capacity of the battery. The battery depreciation process needs to be reduced by conditioning the battery in a suitable manner by controlling its charging and discharging profile, even under various load conditions. In general, the battery life time will be diminished when the battery is operated under a wide range of thermal conditions and frequent charge and deep discharge cycles, particularly at high-pulse current conditions. Batteries are safe, despite reports of explosion or failure, when used with a power-conditioning system that incorporates safety features and automatic shutdown [1]–[5]. Conventional low-cost battery chargers employ few protective features intended for that battery, thus lacking flexibility and full-fledged protection. Hence, BMS, which is flexible to protect batteries of different types and can provide all the safety features, has been the topic of recent development/research in EV [1], [6]–[10] and alternative energy systems [6], [7].

One of the important parameters that are required to ensure safe charging and discharging is SOC. SOC is defined as the present capacity of the battery expressed in terms of its rated capacity [8], [11]–[14]. SOC provides the current state of the battery and enables batteries to safely be charged and discharged at a level suitable for battery life enhancement. Thus, SOC helps in the management of batteries. However, measuring SOC is not direct, because it involves the measurement of

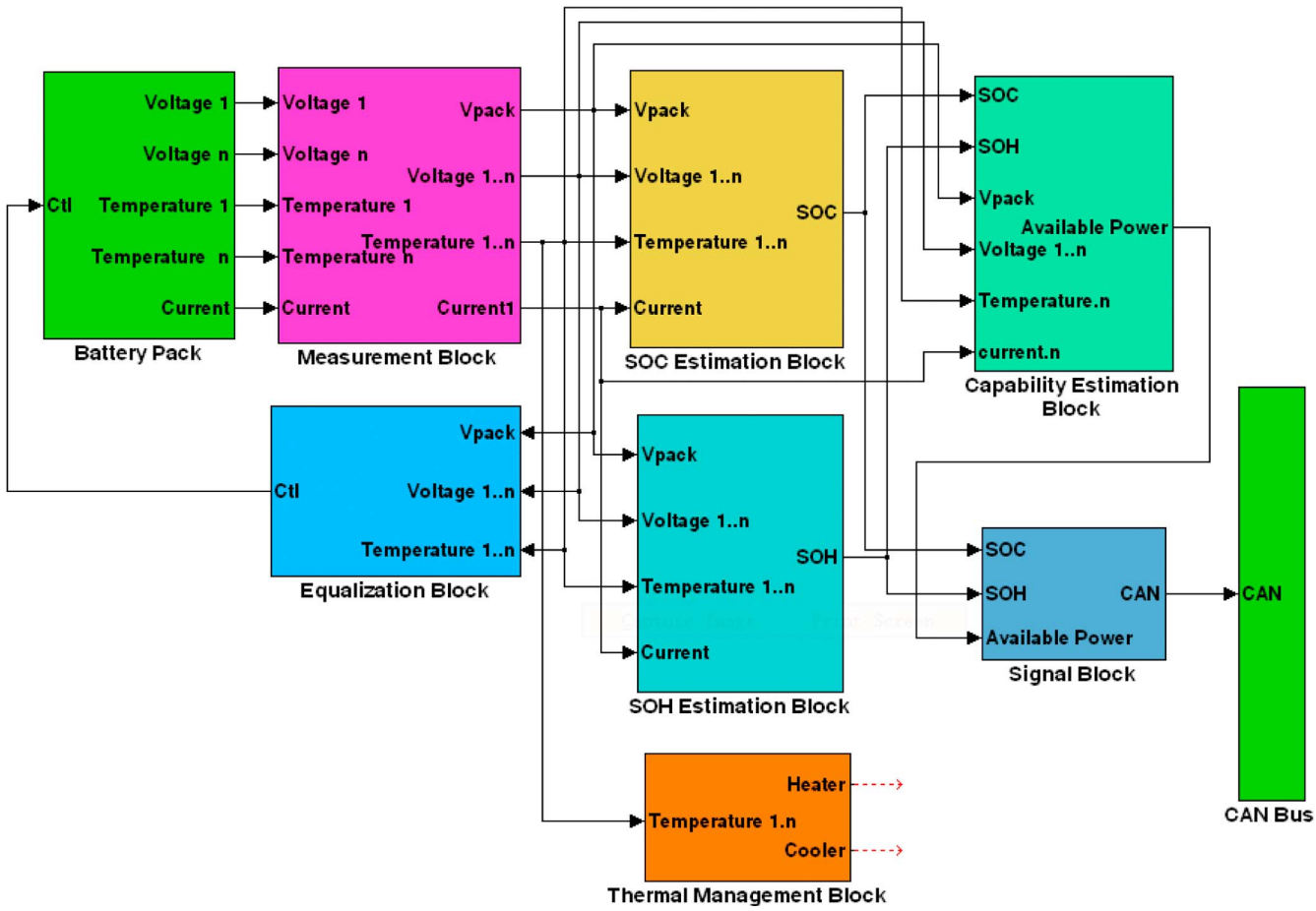

Fig. 1. Block diagram of BMS.

battery voltage, current, temperature, and other information that pertains to the battery under consideration.

Accurate estimation of SOC prevents battery damage or rapid aging by avoiding unsuitable overcharge and overdischarge. The conventional SOC estimation using the Coulomb counting method suffers from error accumulation glitch, leading to inaccurate estimation. In addition, the finite battery efficiency and the chemical reaction that takes place during charge and discharge conditions cause temperature rise, which influences SOC estimation. Therefore, accurate algorithms are needed to model the battery for SOC estimation. In EVs, the number of batteries is connected in series-parallel combination to match the load requirement. Due to manufacturing procedures, not all batteries simultaneously attain full voltage during charging. This condition results in voltage imbalance among different batteries and, consequently, lower capacity from the entire battery string. Therefore, a cell with 100% SOC may not necessarily indicate the actual SOC. Therefore, accurate calculation of SOC must be accompanied by a continuous monitoring of the actual capacity of the cell with a number of measurements of the cells to reflect the actual and practical capability of the cell to fit the different road conditions and driving patterns of EVs.

BMS is a separate entity with hardware and firmware and is connected to a battery charger rather than integrated within the charger. BMS consists of a number of sensing devices for monitoring battery parameters that will be used in the algorithm for SOC estimation. The significant block of any BMS is the battery model block, which requires detailed understanding of battery characteristics for accurate SOC estimation [15], [16]. The model is generally derived from the charging and discharging curves of the battery. One advanced battery model [17] based on a state-space technique is implemented in this paper.

The paper is organized as follows. The proposed BMS is discussed in Section II, The SOC estimation technique is presented in Section III. Experimental results on the chosen LiFeO4 is carried out in Section IV, and the simulation results are discussed in Section V, followed by conclusions in Section VI.

II. Battery-Management System Representation

The block diagram of the proposed BMS is given in Fig. 1, and the functional details of each of the blocks are described as follows.

A. Measurement Block

The measurement block (see Fig. 1) captures individual cell voltages, battery current, and battery temperature at different points of the battery bank, as well as the ambient temperature, and converts them into digital values. All of these data are

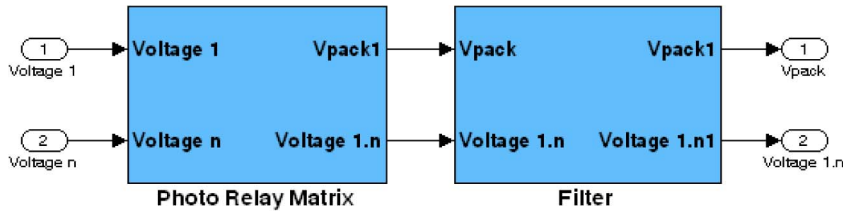

Fig. 2. Cell voltage measurement.

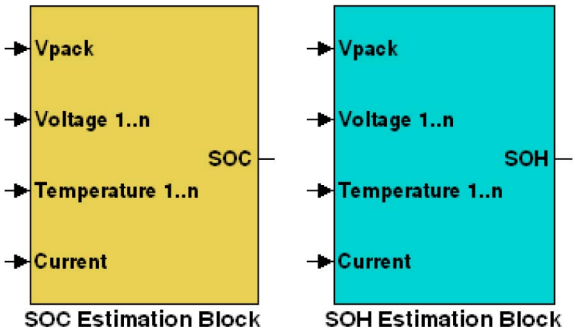

Fig. 3. SOC and SOH estimation block.

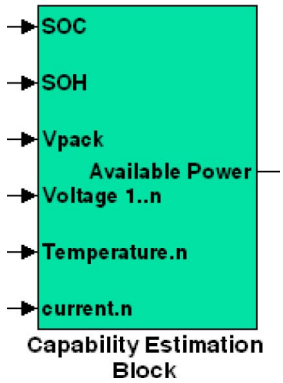

Fig. 4. Demand management block.

then used to estimate the battery status in later stages. The cell voltage measurement block that is shown in Fig. 2 includes a photo relay matrix. In every sample period, only one of the cell voltages is connected to the analog-to-digital (A–D) interface of the central processing unit. The advantage of measuring individual cell voltages justifies the added cost of hardware because it enables cell balancing and overcharge protection at the cell level.

B. Battery Algorithm Block

The battery algorithm block (see Fig. 3) is a conditional status block of the battery. Its principal function is to estimate SOC and SOH using the measured battery variables such as battery voltage, current, and temperature. SOC is defined as the capacity of a battery, expressed as a percentage of its rated capacity. It looks like the "fuel gauge" of vehicle, but it indicates the energy left in the battery. The estimation of SOC is very useful to know the remaining capacity of a battery when the battery is discharged. This condition will permit the estimation of travelling distance of an EV from the available capacity of the battery. SOC is influenced by the temperature, operating cycles, and discharge rate; therefore, BMS should incorporate a model of the battery that takes into account the effects of these factors to deduce SOC. Typical inputs to the model include the voltage, current, and temperature, and they are obtained by the respective sensors. The sensors provide the analog inputs, which are digitized using A–D converters. The inputs are constantly monitored at regular intervals by the microprocessor.

The SOC indication is useful not only to estimate the running distance but, in addition, to keep the batteries at a specified SOC to deliver and accept charging without the risk of overdischarge or overcharge of the cells. In a typical EV, the cells are often subjected to charge dumping due to regenerative braking, leading to the overcharging of the cells, particularly when the SOC of the battery is high. In such events, the BMS should monitor the SOC and control the charge dumped into the battery during regenerative braking to prevent the cells from getting overcharged.

SOC is one of the most important outputs of BMS. There are a few techniques that determine SOC based on cell voltages, currents, and temperature. The most primitive method is direct measurement, i.e., measure either OCV or loaded cell voltage and then deduce the SOC from prestored discharge characteristics. This method does not work well on Li-ion batteries, because the middle section of the discharge curve of Li-ion batteries is very flat. A small measurement error will cause a large variation in SOC. Direct measurement does not take temperature and aging effects into consideration.

C. Capability Estimation Block

After SOC and SOH are determined, BMS has to deduce the maximum charge and discharge current at any instant in accordance with an algorithm. The output of this block is provided to the vehicle ECU so that the battery is not subjected to charge or discharge beyond the specified limits.

The function of the capability estimation block (see Fig. 4) is to send information to the ECU about the present safe level of charging and discharging current of the battery. This information is very vital for the safe operation of the battery and prevents accidental violations of battery specifications.

The control laws for deriving the maximum discharge and charge current based on the inputs are shown in Figs. 5 and 6, which depict the relation between the permissible charge and discharge currents, expressed in terms of the maximum charge/discharge current for various values of different battery parameters. The charge/discharge factors in Figs. 5 and 6 are the permissible charge/discharge currents, expressed in terms of maximum charge and discharge currents, respectively. (The

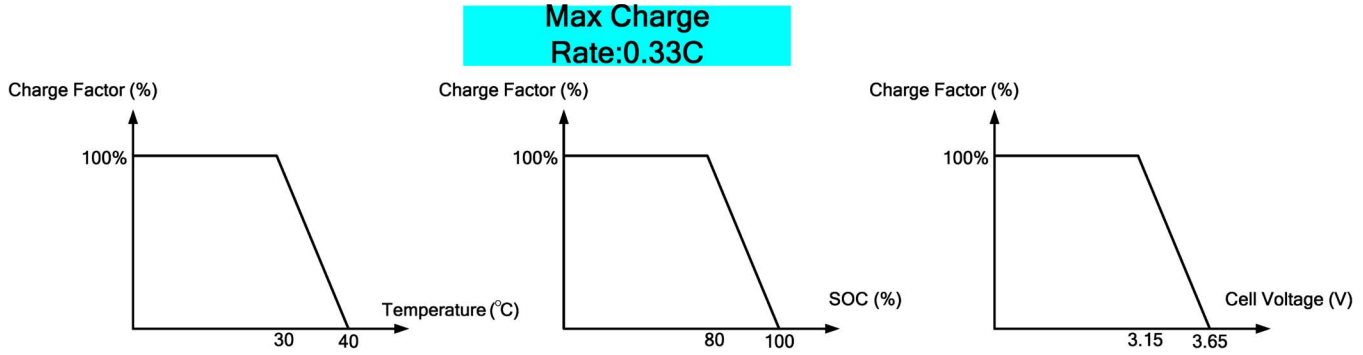

Fig. 5. Effect of inputs on the maximum charge current.

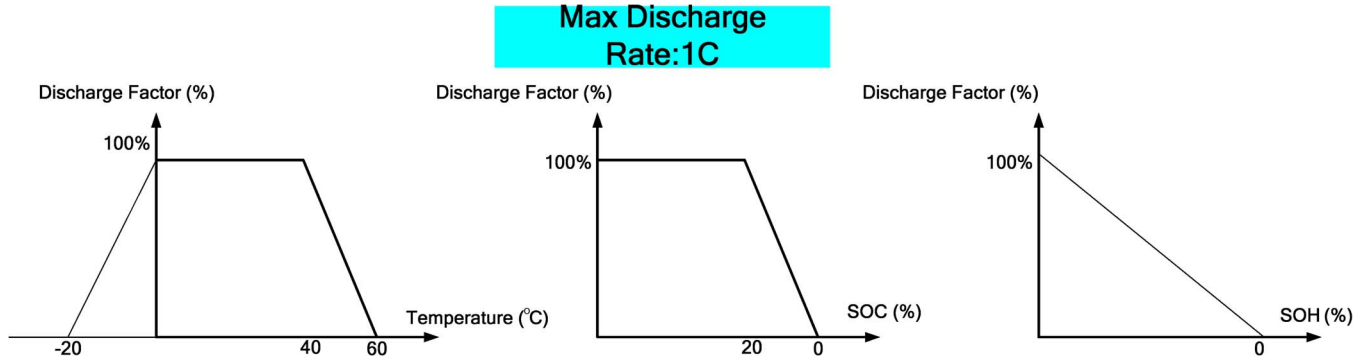

Fig. 6. Effect of inputs on the maximum discharge current.

charging factor is the percentage of the maximum charging current.)

According to the plots in Fig. 5, the BMS will restrict the charging current according to a function that depends on the temperature, SOC, and cell voltage. For example, the charging current has to be decreased if the temperature is in the range of 30 °C–40 °C. Similarly, the maximum current with which the battery can be charged is a function of the SOC and cell voltage.

Note that, according to battery specifications, it is not advisable to discharge the battery at the minimum specified temperature, i.e., less than −20 °C. In practice, the C rate would be very low. The maximum discharge and charge rates are stated in the battery manufacturer's datasheet. It is expressed in C—the nominal capacity of the battery.

D. Cell Equalization Block

Due to the limitation of current manufacturing processes, all cells are not alike. The variation in cell capacity within the range of a few percent up to 15% is common. Other variations such as internal resistance and charge/discharge characteristic are unavoidable. Cell balancing is vital to maximize the usable battery pack capacity and lifetime.

This module compares the cell voltages and finds the difference between the highest voltage cell and the lowest voltage cell (see Fig. 7). If the difference is larger than a preset threshold, then the charging is halted, and the highest voltage cell is discharged through the discharge resistor. The discharge ends once the difference diminishes. This approach is called dissipative cell balancing. Another cell balancing technique is active balancing, which either charges each cell through separate

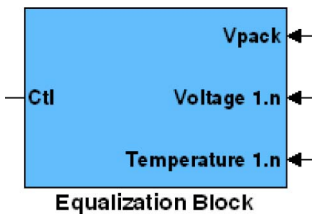

Fig. 7. Cell equalization.

chargers or transfers the charge from the highest voltage cell to the lowest voltage cell. Active balancing is clearly superior in terms of performance and energy efficiency, but its cost is also prohibitive in the cost-sensitive automotive industry.

Many complex battery equalization circuits in the literature [18] use flying capacitors, dc–dc converters with multiple secondary windings, and a single dc converter that can charge the weakest cell in a battery pack. The cost of implementation depends on the equalization time, which, in turn, depends on the power rating of an auxiliary power supply.

E. Thermal Management Block

The boundary diagram of the thermal management block in BMS estimates the battery temperature and is shown in Fig. 8. The temperature estimation is based on a very simple 1-D temperature-estimation method [16]. Thermal management refers to monitoring and controlling the battery temperature so that the battery is not harmed by very high or very low temperature. The outputs of this block control a fan and an electric heater, which attempt to keep the battery temperature within the optimal range.

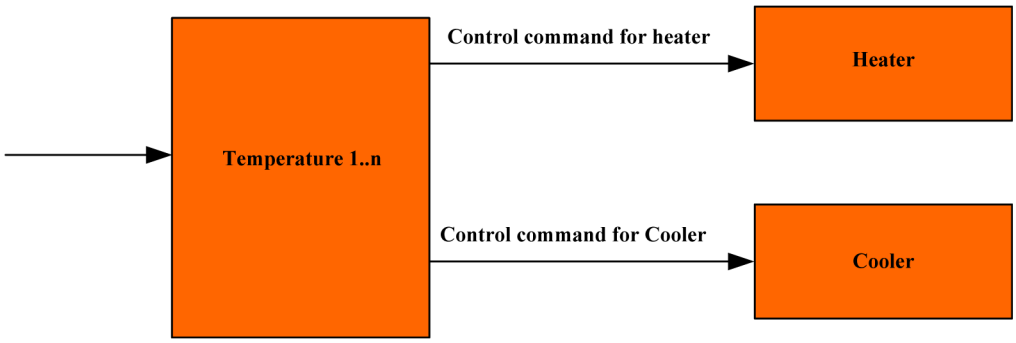

Fig. 8. Thermal management block.

The thermal management block reads ambient and battery temperatures, initiates cooling or heating operation, and sends an emergency signal to ECU in case of abnormal rise in temperature.

III. State of Charge Estimation

The model developed in this paper is based on the state-space method presented in [16], in which SOC is a state of the system, and OCV is predicted using polynomial equations. The predicted OCV is then used for calculating the terminal voltage of the battery, and the calculated terminal voltage is compared with the actual battery voltage. The error between the calculated and the real battery voltage is then used to calculate the filter gain in the Kalman filter to update the state SOC. Thus, the model is used to estimate the SOC of a battery. The battery model simulates a battery control strategy for EV. In this model, the battery SOC is simulated. The parameters represented in the model were extracted from the experiment data of the chosen $LiFePO_4$ battery.

SOH is defined in terms of the percentage of nominal capacity. Aging and charge–discharge cycles are two major factors that reduce the SOH of a battery. The SOH of an average Li-ion battery is reduced to 80% after 1000 charge–discharge cycles. The commonly used method is given by

$$\text{SOH} = \frac{\text{nominal capacity} - \text{loss of capacity}}{\text{nominal capacity}}. \tag{1}$$

A. Battery Model

The battery model [15] shown in Fig. 9 consists of a controlled voltage source in series with a resistor that represents the internal resistance of the cell.

The controlled voltage source is implemented using the following expression:

$$OCV = E_0 - K\frac{Q_R}{Q_R - it} + Ae^{-bit}. \tag{2}$$

The main advantage of this model is that all the parameters can be obtained from the cell's discharge characteristics to represent a particular battery type. The SOC for step changes in load can be derived using

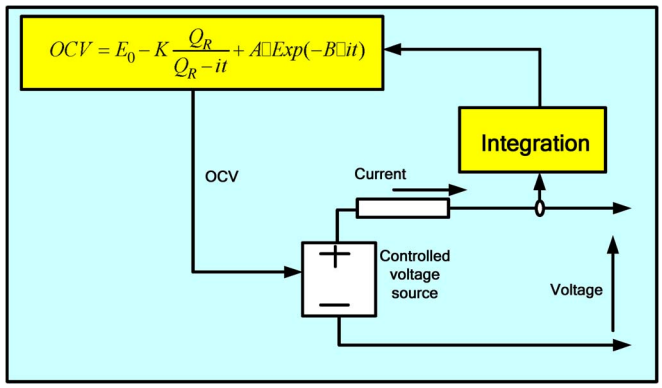

Fig. 9. Generic battery model in [15].

$$SOC_{new} = SOC_{old} - \Delta SOC$$
$$SOC_{new} = SOC_{old} - \frac{i_{new}\Delta t}{Q_R}. \tag{3}$$

The input to the SOC estimation block is the current, and the output is the SOC estimation.

The simple generic model shown in Fig. 9 does not consider the effect of temperature and the rate of discharge current, and hence, the results are not accurate for practical implementation. It lacks the accuracy demanded in a practical application. The following section gives the development of a model based on state-space equations where SOC and SOP are considered as state variables.

B. State-Space Model

The state-space representation of a typical battery [17] is given in (4), shown at the bottom of the next page. The battery terminal voltage is defined in

$$V_{bat}(\mathrm{k}) = OCV\left(S_{oc}(k)\right) + S_{op}(k) + R_n i_k. \tag{5}$$

OCV is obtained by modeling the curve that depicts the relation between SOC and OCV as in

$$OCV\left(\hat{\mathrm{S}}_{\mathrm{oc}}(k+1)\right) = b(1)\hat{\mathrm{S}}^5_{\mathrm{oc}}(k+1) + b(2)\hat{\mathrm{S}}^4_{\mathrm{oc}}(k+1) + b(3)\hat{\mathrm{S}}^3_{\mathrm{oc}}(k+1) + b(4)\hat{\mathrm{S}}^2_{\mathrm{oc}}(k+1) + b(5)\hat{\mathrm{S}}^1_{\mathrm{oc}}(k+1) + b(6). \tag{6}$$

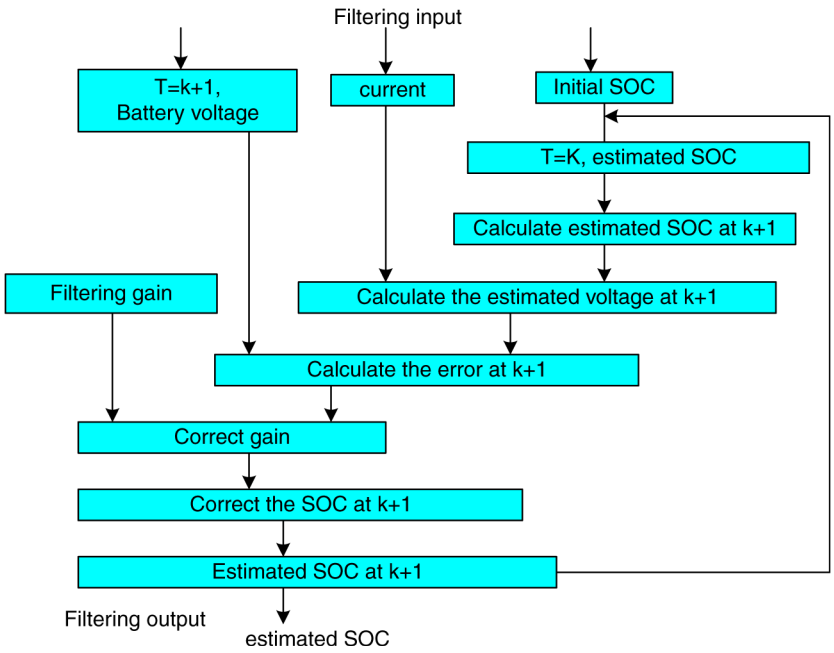

Fig. 10. Flowchart of SOC estimation using the Kalman filtering method.

The following conditions hold.

– M (in volts) depends on the double-layer capacity of the battery as in

$$M = \alpha + \beta \ln |i| + \gamma \Delta S_{oc}. \tag{7}$$

– SOP (in volts) indicates the battery polarization voltage, with a range of $(-M \sim +M)$ and an initial value of 0. We have

$$s(k) = \begin{cases} 1, & i(k) > \varepsilon \\ -1, & i(k) < -\varepsilon \\ s(k-1), & |i(k)| \le \varepsilon. \end{cases} \tag{8}$$

ε is a small positive quantity. In the battery model, (4) is the state equation, where $S_{oc}(k+1)$ is the SOC at discrete-time index $(k+1)$, and $S_{oc}(k)$ is the SOC at discrete-time index (k).

$S_{op}(k+1)$ the SOP at $(k+1)$, $S_{op}(k)$ is the SOP at (k), $i(k)$ is the current when charging or discharging, η_i is the charge or discharge Coulombic efficiency, Δt is the sample period, Q_R is the battery-rated capacity, Q_d is the double-layer capacity (in ampere-hours), M is the maximum polarization voltage (in volts), and $S(k)$ is a sign, which is equal to $+1$ when charging and equal to -1 when discharging. In this equation, $S_{op}(k)$ is treated as a first-order item.

Equation (5) is the output equation, where $V_{bat}(k)$ is the battery terminal voltage, and $OCV(S_{oc}(k))$ is the EMF as a function of SOC. R_n is the internal resistance (in ohms).

Equation (6) represents the EMF as a function of SOC. We use a fifth-order polynomial. In the polynomial, the coefficients of b(1), b(2), b(3), b(4), b(5), and b(6) are used.

Equation (7) represents how we can calculate M, i.e., the maximum polarization voltage. This equation is based on the Tafel formula [19]. Considering the accumulated effect, the Tafel formula is modified by adding an ΔS_{oc} in this paper. ΔS_{oc} is the increment/decrement of S_{oc} during charging or discharging. ΔS_{oc} is reset to 0 when the battery is converted from charge to discharge or from discharge to charge.

C. Battery Algorithm

The battery algorithm block is shown in Fig. 3. The inputs to the block are the battery current, battery voltage, ambient temperature, battery temperature, and module voltage. All of these inputs are obtained by the respective sensors. The total capacity of the battery is the accumulated capacity the battery has charged and discharged since the battery has been used in the vehicle. SOC estimation based on Kalman filtering [20] for a Li-ion battery is used in the SOC estimation algorithm. The flowchart is shown in Fig. 10.

The SOC estimation method involves the following steps.

1) Restore the battery initial SOC.
2) Calculate the battery SOC and SOP according to the state equation in the battery model as in (4).
3) Calculate the battery voltage according to the output equation (5) in the battery model.

$$\begin{bmatrix} S_{oc}(k+1) \\ S_{op}(k+1) \end{bmatrix} = \begin{bmatrix} 1 & 0 \\ 0 & 1 \end{bmatrix} \begin{bmatrix} S_{oc}(k) \\ S_{op}(k) \exp\left(-\left|\frac{i(k)\Delta t}{Q_d}\right|\right) + s_k M \left(1 - \exp\left(-\left|\frac{i(k)\Delta t}{Q_d}\right|\right)\right) \end{bmatrix} + \begin{bmatrix} \left(\frac{\eta_i \Delta t}{Q_R}\right) \\ 0 \end{bmatrix} i(k) \tag{4}$$

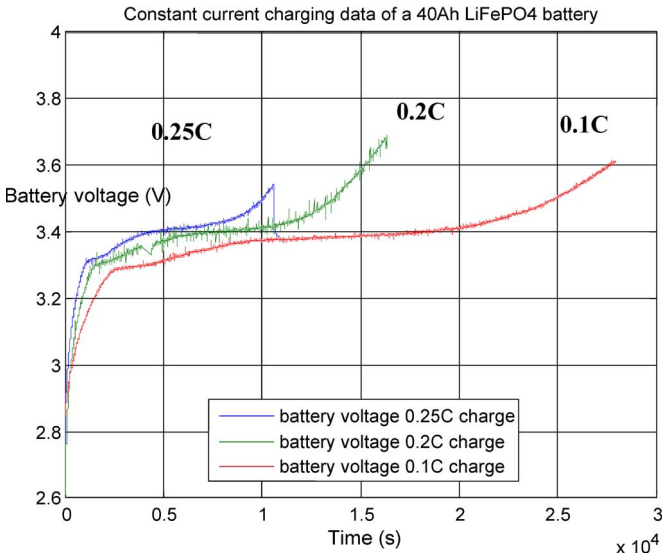

Fig. 11. Constant current charge at 16 °C.

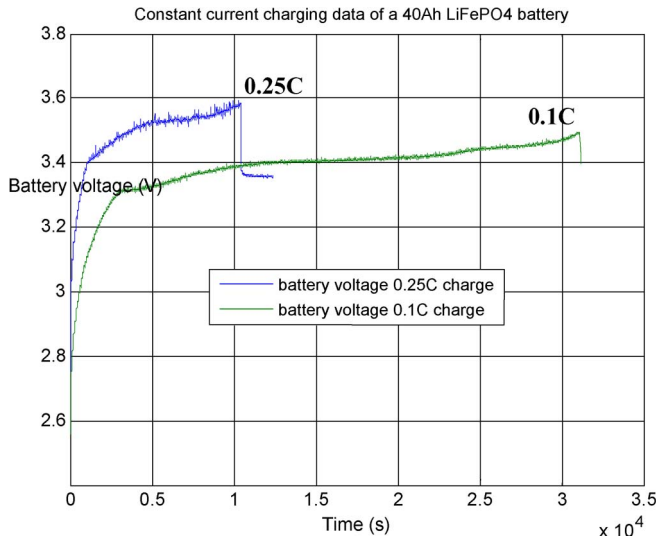

Fig. 12. Constant current charge at 40 °C.

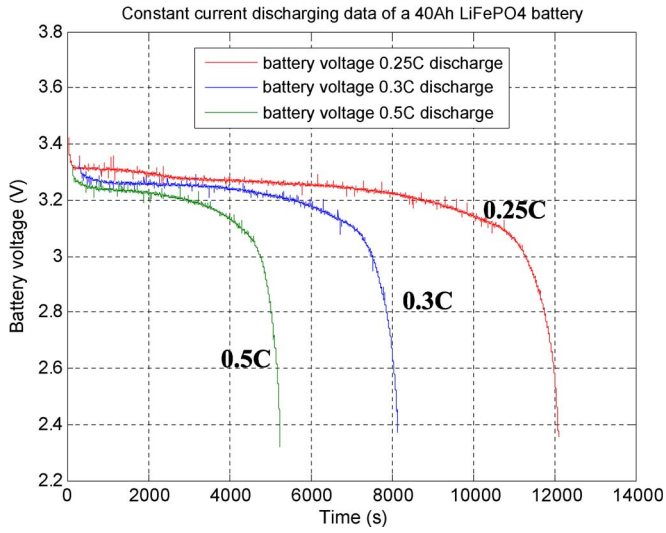

Fig. 13. Constant current discharge at 16 °C.

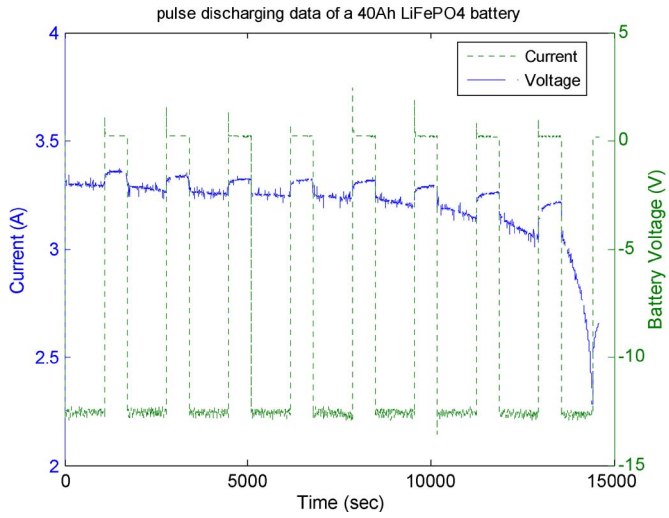

Fig. 14. Pulse discharge at 16 °C.

4) Compare the real battery voltage and the model voltage, and calculate the battery voltage error as

$$\tilde{V}_{bat}(k+1) = V_{bat}(k+1) - \hat{V}_{bat}(k+1). \tag{9}$$

5) Calculate the filtering gain as

$$\begin{aligned} &P(k+1|k) \\ &\quad = \Phi[k+1,k]P(k|k)\Phi^T[k+1,k] \\ &\qquad + \Gamma(k+1,k)Q_k\Gamma^T(k+1,k) \end{aligned} \tag{10}$$

$$\begin{aligned} &P(k+1|k+1) \\ &\quad = P(k+1|k) - P(k+1|k)H^T(k+1) \\ &\qquad \times \left[H(k+1)P(k+1|k)H^T(k+1) + R_{k+1}\right]^{-1} \\ &\qquad \times H^T(k+1)P(k+1|k). \end{aligned} \tag{11}$$

Here, $P(k+1,k)$ means that, in the current interval k, predict P in the next interval $k+1$. Then, $P(k+1,k)$ is calculated with the state equation. The vertical line here is a symbol. In some papers, a "," may be instead used.

$P(k+1,k+1)$ means that, in the current interval $k+1$, predict P in the next interval $k+1$. Then, $P(k+1,k+1)$ is calculated with the output equation.

Therefore, in the SOC algorithm, to be precise, P means the estimated SOC error.

The heart of the solution is a set of computationally efficient recursive relationships that involve both an estimate of the state itself and the covariance matrix $P(k)$ of the state estimate error.

$P(k)$ is the state error covariance matrix, assuming that $P(0|0) = 0.3$ (the initial SOC error).

$\Phi(k+1,k)$ is the coefficient matrix in this algorithm, with $\Phi(k+1,k) = 1$.

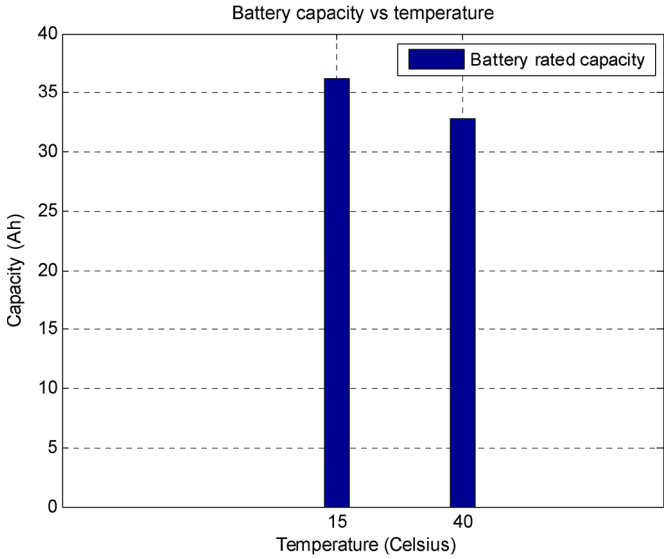

Fig. 15. Battery-rated capacity.

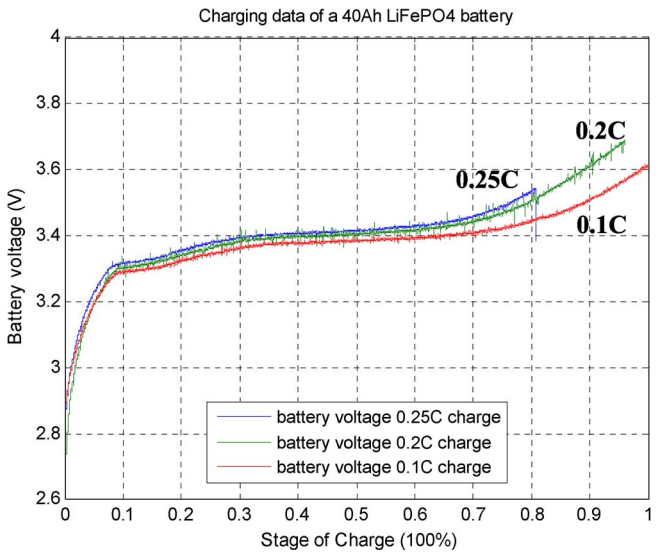

Fig. 16. Charging data of a 40-Ah $LiFePO_4$ battery at 16 °C.

Assume that w and v are stochastic noise processes. In addition, w and v are mutually uncorrelated white Gaussian random processes, with zero mean and covariance matrix.

Q is the covariance of w and is decided according to the current sample error.

For example, the following conditions hold.

- The current sample circuit error is 0.5 A.
- The sample period is 2 s.
- The battery-rated capacity is 40 Ah.
- $\mathrm{Q} = (0.5 * 2)/(40 * 3600)$.
- R is the covariance of v and is decided according to the voltage sample relative error.
- H is the coefficient matrix in the output equation.
- $\Gamma(\mathrm{k}+1, \mathrm{k})$ is the coefficient matrix of stochastic noise w.

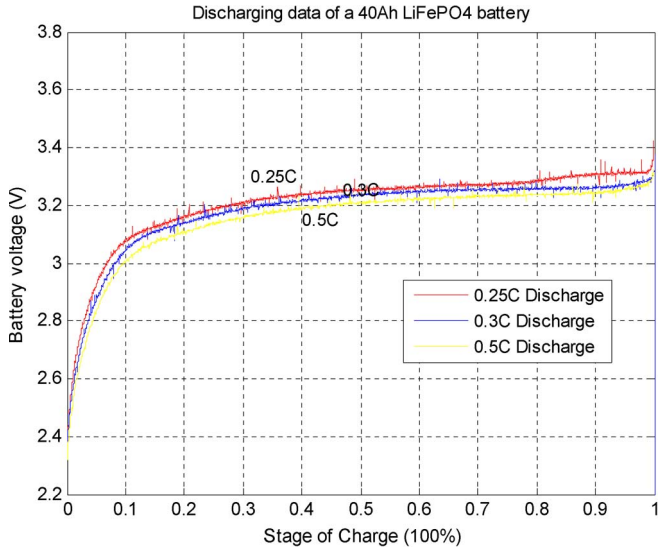

Fig. 17. Discharging data of a 40-Ah $LiFePO_4$ battery at 16 °C.

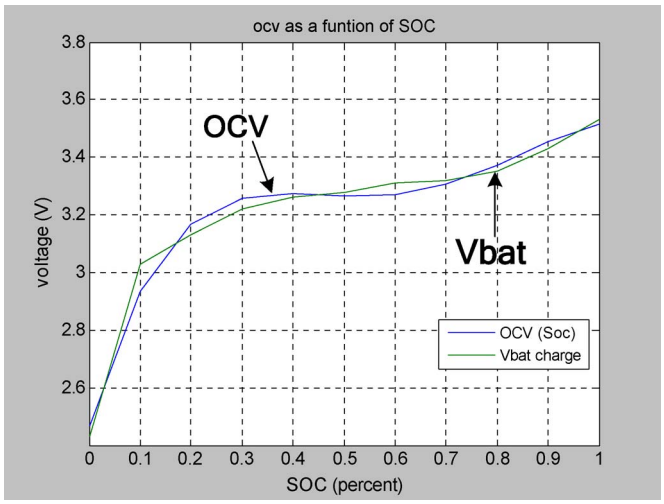

Fig. 18. Battery OCV versus SOC.

6) Calculate the SOC correction gain as

$$K(k+1) = P(k+1|k)H^T(k+1) \times \left[H(k+1)P(k+1|k)H^T(k+1) + R_{k+1}\right]^{-1}. \quad (12)$$

Following the output measurement equation, the state error covariance matrix $\mathrm{P}(\mathrm{k}+1|\mathrm{k})$ and the coefficient matrix in the output equation are used to calculate the SOC correct gain.

7) Correct the battery SOC as follows:

$$\hat{S}_{oc}(k+1|k+1) = \hat{S}_{oc}(k+1|k) + K(k+1)\tilde{V}_{bat}(k+1). \quad (13)$$

The correct gain would add to the SOC calculation. If the battery voltage error and the SOC correct gain is large, the SOC update tends to be large. In practice, the correct $K(k+1)\tilde{V}_{bat}(k+1)$ should not be more than $(-1\%$ to $1\%)$ in one sample period; otherwise, the vehicle control strategy may be influenced.

8) Output SOC and return to step 2).

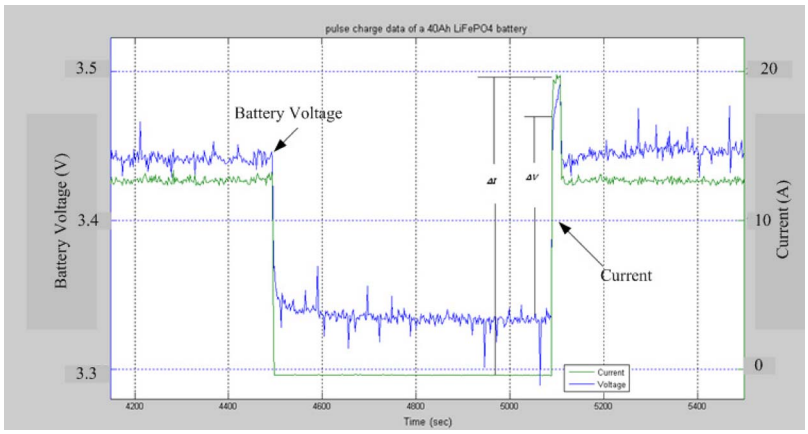

Fig. 19. Step load change experiment to obtain internal resistance.

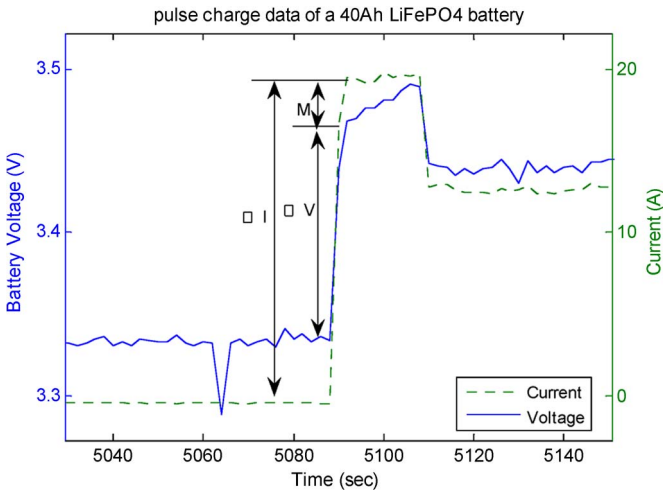

Fig. 20. Step load change experiment to extract parameters.

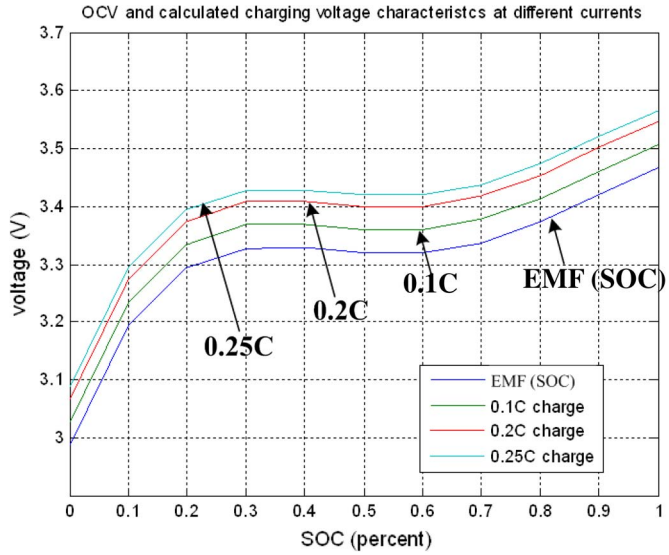

Fig. 21. Battery voltage versus SOC at different charging rates.

IV. Experiments

Several battery experiments have been performed at 16 °C and 40 °C to collect estimate battery parameters and to compare the results from the simulation. The experiments include the following parameters:

- constant current charge;
- constant current discharge;
- pulse current charge;
- pulse current discharge;
- temperature characteristics experiments;
- variable current experiments.

In the constant current charge experiments, the current is 4 A (0.1 C), 8 A (0.2 C), and 10 A (0.25 C), as shown in Figs. 11 and 12. The maximum voltage is 3.6 V. Experimental data are used to calculate the rated capacity of the battery.

As shown in Fig. 11, the voltage suddenly drops when the current is from 0.25 C to 0, which indicates the termination of the charging procedure. It is normal for the voltage to drop during the charging process when the current is reduced or for the voltage to increase during discharge when the current is reduced. In Fig. 11, the experiment at 0.25 C ended at about 3.3 h when the relay has tripped due to a timer circuit. The timer function was included to minimize the danger due to overcharging. As shown in the increasing slope of the voltage curve near the end of discharge, it would have taken the cell just a few more minutes to reach the end of charge voltage of 3.6 V had the charging been continued. Thus, the termination by timer function would lead to insignificant error when the safety issue is considered.

In the constant current discharge experiments, the battery was subjected to current discharge of different C-rates such as 10 A (0.25 C), 13.3 A (0.3 C), and 20 A (0.5 C), and readings were recorded for each set. The end of discharge is when the

TABLE I
Parameters Used for the Simulation

parameters	Value	Unit
Coefficients of OCV-b1	-2.30	
Coefficients of OCV-b2	6.66	
Coefficients of OCV-b3	-6.75	
Coefficients of OCV-b4	2.98	
Coefficients of OCV-b5	2.86	
α	0.020	
β	0.020	
γ	0.018	
R_n	0.007778	Ohm
Q_R	40	Ah
Q_d	1800	Ah

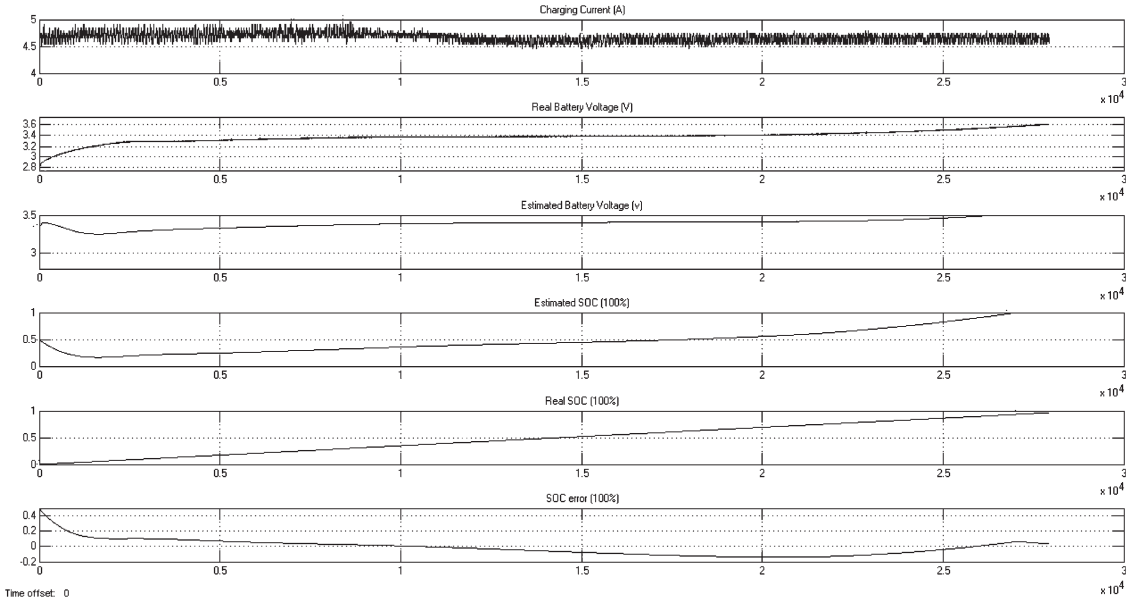

Fig. 22. Results for the 4-A charge. Scope 1: Charging current. Scope 2: Real battery voltage. Scope 3: Estimated battery voltage. Scope 4: Estimated SOC. Scope 5: Real SOC. Scope 6: SOC error.

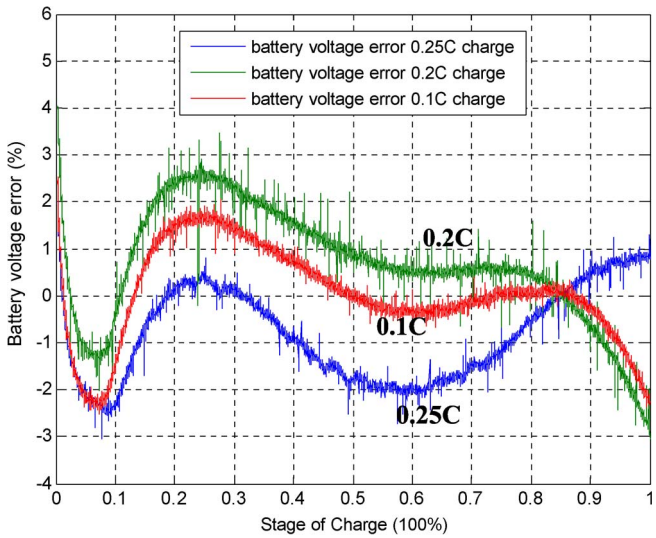

Fig. 23. Error between the computed voltage and the experiment voltage at different charging currents.

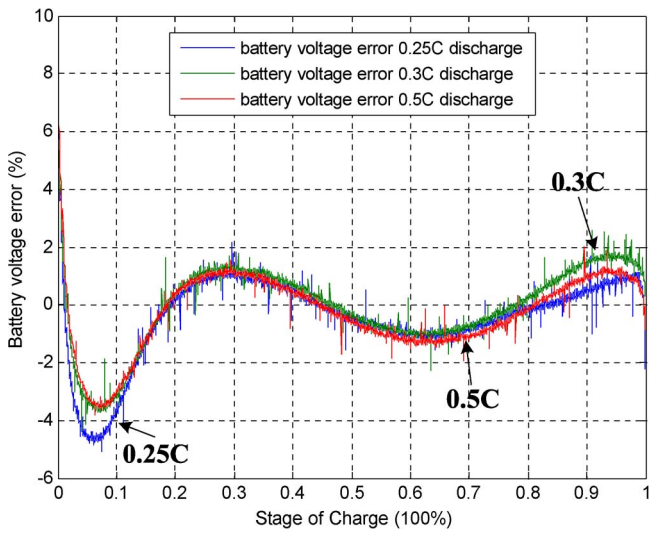

Fig. 24. Error between the computed voltage and the experiment voltage at different discharging currents.

minimum voltage is 2.4 V. The experimental data are used to calculate the rated capacity of the battery. The discharge plots are shown in Fig. 13. The plots from pulse current discharging are shown in Fig. 14. Fig. 15 shows the estimated capacity of the battery at two different temperatures, confirming the drop in the capacity at higher temperature.

A. Estimating the Parameters for the Battery Using Experiments

Experiments are done to extract the parameters of the battery, including constant current charging, constant current discharging, pulse current charging, pulse current discharging, and variable current charging/discharging. Fig. 16 shows the plots of battery voltage versus SOC during charging at 0.1 C, 0.2 C, and 0.25 C. Fig. 17 shows the plots of battery voltage versus SOC during discharge at 0.25 C, 0.3 C, and 0.5 C.

Figs. 16 and 17 are obtained by calculating the SOC from the V–I curve obtained from the experimental results. The results can be used for comparison with the predicted battery voltage from the simulation. The simulation requires a few parameters of the battery model, which can be extracted as follows.

The parameters for the battery model are listed as follows:

1) the coefficients of the polynomial of OCV;
2) battery internal resistance, $\mathrm{R_n}$ (in ohms);
3) battery-rated capacity (in ampere-hours);
4) double-layer capacity, $\mathrm{Q_d}$ (in ampere-hours);
5) polarization coefficients α, β, and γ.

Some of the parameters can be extracted from the experimental data, and the remaining parameters can be extracted from the

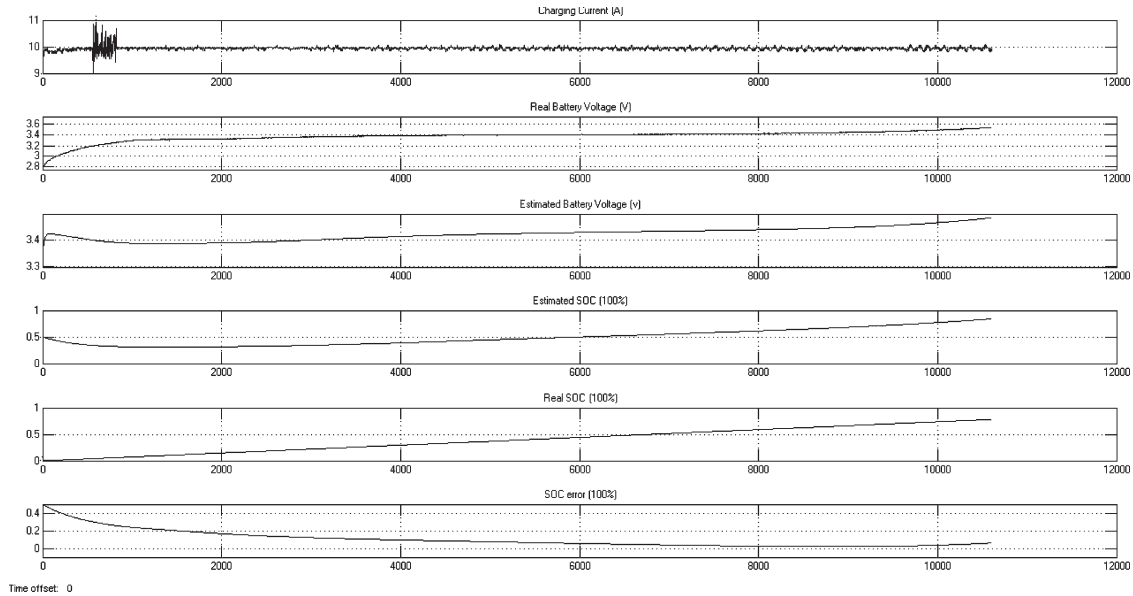

Fig. 25. SOC estimation results for the 10-A charge. Scope 1: Charging current. Scope 2: Real battery voltage. Scope 3: Estimated battery voltage. Scope 4: Estimated SOC. Scope 5: Real SOC. Scope 6: SOC error.

TABLE II
SPECIFICATIONS FOR THE HP-56110160* Li-ION PHOSPHATE BATTERY

NO.	Items		Unit	Value	Remarks
1	Rated Capacity		Ah	40.0	/
2	Nominal Voltage		V	3.15	/
3	Charging		/	CC/CV	/
4	Charge Upper Limit Voltage		V	3.65	/
5	Discharge Cut-off Voltage		V	2.3	/
6	Charging Current		A	13.2	Constant Current
7	Discharging Current		A	40	Constant Current
8	Maximum Discharging Current		A	120	< 15S
9	Weight		kg	1.34±0.01	/
10	Resistance		mΩ	<5	/
11	Dimension (H×W×L)		mm	56×110×160	/
12	Working Temperature	Charging	℃	0 ~ 45	/
		Discharging	℃	-20 ~ 60	/
13	Storage Temperature	1 month	℃	-20 ~ 60	/
		3 months	℃	-20 ~ 45	/
		6 months	℃	-20 ~ 25	/
	Atmospheric pressure		KPa	86 ~ 106	/
	Relative Humidity		RH	25% ~ 85%	/

*Manufacturer: Shandong Hipower New Energy Group Co.,Ltd, China: Products Model HP-56110160

specification of the manufactures. The parameter extractions are explained as follows.

1) For the coefficients of the polynomial in the OCV expression, we have

$$OCV\,(\mathrm{S_{oc}}(k)) = b(1)\mathrm{S}_{\mathrm{oc}}^4(k) + b(2)\mathrm{S}_{\mathrm{oc}}^3(k) + b(3)\mathrm{S}_{\mathrm{oc}}^2(k) + b(4)\mathrm{S}_{\mathrm{oc}}^1(k) + b(5). \quad (14)$$

Based on the charge and discharge experimental data, the V–I data of the battery are obtained. Then, creating a vector, a plot of OCV versus SOC can be obtained, from which a polynomial function can be fitted (see Fig. 18).

2) Based the battery data and using the following equation:

$$R_n = \frac{\Delta V}{\Delta I} \quad (15)$$

the battery internal resistance can be obtained. Fig. 19 shows the charge internal resistance $(3.47 - 3.33)/18 = 0.007778\ \Omega$.

3) The parameter $\mathrm{Q_R}$ is the rated capacity (in ampere-hours) and comes from the battery manufacturer. Because $\mathrm{Q_R}$ is dependent on the battery temperature, it would accordingly be adjusted in a lookup table.

4) $\mathrm{Q_d}$ is the double-layer capacity (in ampere-hours).

Based on the pulse charge or pulse discharge curve, $\mathrm{Q_d}$ is derived from the battery voltage rise time: $\mathrm{Q_d} =$ rise time $*$ current.

5) M is the maximum polarization voltage (in volts) and can be calculated using $M = \alpha + \beta \ln|i| + \gamma \Delta S_{oc}$.

The parameters α and β can be extracted from pulse charge data. Fig. 20 shows M at a 20-A pulse charge curve. In the same way, get another M to calculate the coefficients α and β.

6) The adjustment coefficient γ is an adjustment factor that can be extracted from comparison of the simulation results with real charge and discharge curve.

Fig. 21 shows battery voltage versus SOC at different charging rates. The information can be used to obtain a function that relates the SOC and the OCV to predict the terminal voltage of the battery.

V. Simulation in Simulink

A simulation was conducted to simulate charging at 4 A of the $\mathrm{LiFePO_4}$ cell at 16 °C. The parameters of the simulation are given in Table I. The initial SOC of the cell was zero. To examine the capability of the algorithm to track the real SOC, the initial SOC of the cell in the simulation was set at 50%. Fig. 22 shows the results of the simulation under 4-A charging. Scope 1 shows that the charge current is 4 A, scope 2 shows the battery voltage, and scope 3 shows the calculated voltage. Scope 4 shows the calculated SOC, scope 5 shows the real SOC, and scope 6 shows the SOC error.

Based on scope 6, we can see that the error between the simulated and the true SOC diminishes as the simulation progresses, confirming the capability of the algorithm.

The simulation runtime is 27 942 s, and the parameters used for simulation is set as shown in Table I.

The percentage of error between the experimental and the simulated results are shown in Fig. 23 for charging and in Fig. 24 for discharging. The small error confirms the ability of the Kalman filter to accurately predict the SOC and the battery voltage.

Another simulation is carried out to test the SOC estimation algorithm. Accordingly, the battery is charged with 10 A and with an initial SOC setting of 0.5, but the true SOC of the battery was 0. Fig. 25 shows the simulation results during charging. After Kalman filtering (about 2000 s later), the estimated SOC becomes equal to the real SOC, thus proving the dynamic adjustability of the Kalman filtering method.

VI. Conclusion

In this paper, the functional blocks of a BMS have been developed. The various functional blocks, e.g., battery model, thermal management, and battery capability estimation, are integrated and simulated in the Simulink platform. The SOC estimation has been implemented using Coulomb counting with the SOC reset mechanism using the OCV method, thereby eliminating the limitation of the stand-alone Coulomb counting method. The Kalman filtering technique was used to improve the SOC estimation technique. The application of the Kalman filtering method in the battery algorithm significantly improves the accuracy of the SOC estimation, which is verified by experimental and simulation results.

Appendix

Table II shows the specifications for the HP-56110160 Li-ion phosphate battery.

Acknowledgment

The authors would like to thank the Automotive Parts and Accessory Systems R&D Centre Limited (APAS), Hong Kong, particularly J. Xu, M. Haibo, W. Ting, H. Bufu, and C. H. Leung, for their technical support.

References

[1] C. R. Gould, C. M. Bingham, D. A. Stone, and P. Bentley, "New battery model and state-of-health determination through subspace parameter estimation and state-observer techniques," *IEEE Trans. Veh. Technol.*, vol. 58, no. 8, pp. 3905–3916, Oct. 2009.

[2] Y.-J. Lee, A. Khaligh, and A. Emadi, "Advanced integrated bidirectional AC/DC and DC/DC converter for plug-in hybrid electric vehicles," *IEEE Trans. Veh. Technol.*, vol. 58, no. 8, pp. 3970–3980, Oct. 2009.

[3] H. L. Chan, K. W. E. Cheng, and D. Sutanto, "Phase-shift controlled DC–DC converter with bidirectional power flow," *Proc. Inst. Elect. Eng.—Elect. Power Appl.*, vol. 148, no. 2, pp. 193–201, Mar. 2001.

[4] L. Solero, "Nonconventional on-board charger for electric vehicle propulsion batteries," *IEEE Trans. Veh. Technol.*, vol. 50, no. 1, pp. 144–149, Jan. 2001.

[5] A. Szumanowski and Y. Chang, "Battery management system based on battery nonlinear dynamics modeling," *IEEE Trans. Veh. Technol.*, vol. 57, no. 3, pp. 1425–1432, May 2008.

[6] S. Duryea, S. Islam, and W. Lawrance, "A battery management system for stand-alone photovoltaic energy systems," *IEEE Ind. Appl. Mag.*, vol. 7, no. 3, pp. 67–72, Jun. 2001.

[7] B. Hauck, BATTMAN—A Battery Management System, Milan, Italy, 1992.

[8] A. Affanni, A. Bellini, G. Franceschini, P. Guglielmi, and C. Tassoni, "Battery choice and management for new-generation electric vehicles," *IEEE Trans. Ind. Electron.*, vol. 52, no. 5, pp. 1343–1349, Oct. 2005.
[9] R. Peng and M. Pedram, "Battery-aware power management based on Markovian decision processes," *IEEE Trans. Comput.-Aided Design Integr. Circuits Syst.*, vol. 25, no. 7, pp. 1337–1349, Jul. 2006.
[10] A. Mills and S. Al-Hallaj, "Simulation of passive thermal management system for lithium-ion battery packs," *J. Power Sources*, vol. 141, no. 2, pp. 307–15, Mar. 1, 2005.
[11] Z. Yang, H. Hao, X. Guoqing, and Z. Zhiguo, "Hardware-in-the-loop simulation of pure electric vehicle control system," in *Proc. Int. Asia Conf. CAR*, 2009, pp. 254–258.
[12] L. Maharjan, S. Inoue, H. Akagi, and J. Asakura, "State-of-charge (SOC)-balancing control of a battery energy storage system based on a cascade PWM converter," *IEEE Trans. Power Electron.*, vol. 24, no. 6, pp. 1628–1636, Jun. 2009.
[13] H. Dai, X. Wei, and Z. Sun, "Model-based SOC estimation for high-power Li-ion battery packs used on FCHVs," *High Technol. Lett.*, vol. 13, no. 3, pp. 322–326, 2007.
[14] J. Lee, O. Nam, and B. H. Cho, "Li-ion battery SOC estimation method based on the reduced order extended Kalman filtering," *J. Power Sources*, vol. 174, no. 1, pp. 9–15, Nov. 2007.
[15] *MATLAB/Simulink User's Guide*, The MathWorks Inc., Natick, MA, 2007.
[16] S. Gold, "A PSPICE macromodel for lithium-ion batteries," in *Proc. Battery Conf. Appl. Adv.*, 1997, pp. 215–222.
[17] G. L. Plett, "Kalman-filter SoC estimation for LiPB HEV cells," in *Proc. 19th Int. Battery, Hybrid, Fuel Cell EVS*, Busan, Korea, 2002, pp. 527–538.
[18] J. Cao, N. Schofield, and A. Emadi, "Battery balancing methods: A comprehensive review," in *Proc. IEEE VPPC*, Harbin, China, Sep. 3–5, 2008, pp. 1–6.
[19] A. J. Bard and L. R. Faulkner, *Electrochemical Methods: Fundamentals and Applications*, 2nd ed. New York: Wiley, 2001.
[20] R. E. Kalman, "A new approach to linear filtering and prediction problems," *Trans. ASME, J. Basic Eng.*, vol. 82, pp. 35–45, 1960.

K. W. E. Cheng (M'90–SM'06) received the B.Sc. and Ph.D. degrees from the University of Bath, Bath, U.K., in 1987 and 1990, respectively.

Before joining the Hong Kong Polytechnic University in 1997, he was with Lucas Aerospace, U.K., as a Principal Engineer, where he led a number of power electronics projects. He is currently a Professor and the Director of the Power Electronics Research Centre and the Department of Electrical Engineering, Hong Kong Polytechnic University. He has published more than 250 papers and seven books. His research interests include power electronics, motor drives, electromagnetic interference, electric vehicles, and energy saving.

Dr. Cheng received the IEE Sebastian Z. De Ferranti Premium Award (1995), an outstanding consultancy award (2000), the Faculty Merit Award for Best Teaching (2003) from the University, the Faculty Engineering Industrial and Engineering Services Grant Achievement Award (2006), the Brussels Innova Energy Gold Medal with Mention (2007), the Consumer Product Design Award (2008), and the Electric Vehicle Team Merit Award of the Faculty (2009).

B. P. Divakar received the M.E. degree in power systems from Annamalai University, India in 1991 and the Ph.D. degree in power electronics from the Hong Kong Polytechnic University, Kowloon, Hong Kong, in 1998.

He has more than 16 years of teaching and research experience. He is currently a Professor with the Department of Electrical and Electronics Engineering, Reva Institute of Technology and Management, Bangalore, India. His research interests include soft switching of converters, power factor controllers, chargers, battery-management systems, power quality, electromagnetic interference, and high intensity discharge lightings.

Hongjie Wu received the Ph.D. degree from Beihang University, Beijing, China, in 2006.

Before joining the Shanghai Jiao Tong University, Shanghai, China, in 2008, he held a postdoctoral position with Beihang University, where he led a number of battery-management system projects through the National High-Tech Research and Development Program (863 Program). He is currently a Research Fellow with the National Engineering Laboratory of Automotive Electronics, Shanghai Jiao Tong University. He has published more than 15 papers. He is the holder of three patents. His research interests include energy-storage systems for electric vehicles or power stations, particularly battery-management systems, ultracapacitors, and hardware-in-the-loop (HIL) test systems.

Kai Ding received the B.E., M.E., and Ph.D. degrees from Huazhong University of Science and Technology, Wuhan, China, in 1998, 2001, and 2004, respectively.

He is currently a Research Fellow with the Power Electronics Research Centre, Department of Electrical Engineering, Hong Kong Polytechnic University, Kowloon, Hong Kong. His research interests include multilevel converters, fuel cell techniques, electrical vehicles, battery-management systems, dynamic voltage restorers, power electronics applications in electric power systems, and computer simulation.

Ho Fai Ho received the B.Eng. and Ph.D. degrees from the Hong Kong Polytechnic University, Kowloon, Hong Kong, in 1998 and 2005, respectively.

He is currently a Research Associate with the Department of Electrical Engineering, the Hong Kong Polytechnic University. His research interests include intelligent control, adaptive control, and power converter control.